Observations of pulsating Marangoni phenomena during the local oxidation of deoxidized liquid steel

The Royal Society

| **Email alerting service** | Receive free email alerts when new articles cite this article - sign up in the box at the top right-hand corner of the article or click **here** |

The Royal Society

Observations of pulsating Marangoni phenomena during the local oxidation of deoxidized liquid steel

By G. R. Belton, T. J. Evans and L. Strezov

*BHP Research, Newcastle Laboratories, PO Box 188,
Wallsend, NSW 2287, Australia*

Studies have been made by means of a high-speed video technique of the surface of Al–Si–Mn deoxidized liquid steel at about $1600\,^\circ$C during local reoxidation by gently impinging flows of CO_2-containing gases. Expanding 'necklaces' of alumina oxidation product have been observed to form at frequencies of up to about 5 Hz and to travel at velocities of up to $250\,\mathrm{mm\,s^{-1}}$ near to the gas inlet tube, depending on the experimental conditions. The pulsation frequency appears to be controlled by the rate of diffusion of aluminium to the surface. The effects of additions of the surfactants sulphur and selenium on the velocity of the moving front are shown to be consistent with the processes being surface tension driven.

Keywords: Marangoni flow; steel reoxidation; surface velocities;
effect of surfactants; local oxidation; alumina formation

1. Introduction

Thermodynamic and kinetic phenomena at the gas–solid, gas–liquid, solid–liquid, liquid–liquid and liquid 1–liquid 2–solid interfaces are pervasive in iron and steel making. Olette (1993) expressed this succinctly in the title of his Yukawa Memorial Lecture, 'Surface phenomena: a cornerstone of iron and steel making processes', in which he discussed several important examples where interfacial behaviour is a determining factor. Studies of Marangoni effects in particular have been reviewed by Hammerschmid (1987) and, more recently, by Mukai (1992). The often profound effects of surface-active elements on the rates of interfacial reactions of gases with liquid iron and its alloys have also been reviewed recently by Belton (1993).

The present paper reports and discusses observations of concentration-driven Marangoni-induced pulsating flows which occur during the oxidation of aluminium-containing deoxidized steel by gently impinging flows of oxidizing gases under essentially isothermal conditions. The work was undertaken as part of broader studies of the phenomena which lead to disturbances of the meniscus at the liquid steel–gas-mould interface in the strip casting of steel. In particular, the studies are of initially manganese–silicon deoxidized steel with additions of aluminium. The results are also of possible interest in understanding the phenomena which lead to the blockage of submerged entry nozzles by agglomerated alumina particles.

2. Experimental details

About 135 kg of liquid steel was contained within a 300 mm internal diameter magnesia crucible in an induction furnace. By using this large mass, the temperature of the steel decreased only slowly from about 1600 to 1580 °C over a period of 4–5 minutes, when the induction power was switched off. The melt was sealed against the atmosphere by means of a refractory-coated steel plate and dense fibrous refractory gasket. The bulk atmosphere was provided by flowing a 5% H_2–Ar gas mixture through a tube in the steel plate, with provision of a restricted outlet. The oxidizing gas mixture was introduced through a vertical 5 mm bore alumina tube, with the tip held at about 5 mm above the liquid metal surface. In one series of experiments, pure CO was passed through a second tube which was similarly positioned at a lateral distance of 50 mm, centre to centre, from the first. In other experiments, the second tube was dispensed with. Temperature measurement was by means of an alumina-sheathed noble metal thermocouple inserted in the liquid metal, and the flow rates of the high purity gases were controlled by mass flow meters. Sampling of the melt for chemical analysis was through a sealable port in the cover plate.

Observation and recording of the events occurring on the surface of the liquid steel was by means of a high-speed video camera sighted through an optical flat cemented on a sight tube in the steel cover plate. Several optical filters were tried, but the most suitable was found to be a lens from a pair of arc-welding goggles. Reduction of the glare was also found to be assisted by making the refractory lining of the steel cover plate convex rather than flat.

The studies were carried out with melts which had been prepared for other experiments, and hence were manganese–silicon deoxidized low-carbon (0.001–0.07 wt% C) steels. Aluminium was added through the sampling port, the system closed, and the 5% H_2–Ar bulk atmosphere gas passed at a flow rate of about $5 \, l \, min^{-1}$. The reaction gases were introduced through one or both of the 5 mm bore inlet tubes. After the initial alumina oxidation product had cleared from the surface, and following stabilization of the temperature at 1600 °C, the power to the induction furnace was turned off and observations begun. Video recording, at 25–500 frames per second, was typically begun after about a further 30 s. Observations were concluded when the temperature had decreased to about 1580 °C.

Quantitative measurements of pulsation frequencies and velocities were essentially manual, i.e. through repeated replaying of the video tapes at various speeds and counting, and by measurement of the distances moved in successive frames.

3. Observations and results

(*a*) *High aluminium-content melts with an oxidizing gas flow rate of about* $100 \, ml \, min^{-1}$

The compositions of the melts for three successive sets of experiments were: 0.0190 ± 001 wt% Al, 0.071–0.074 wt% C, 0.039–0.042 wt% S, 0.32 wt% Mn and 0.048–0.057 wt% Si. The oxidizing gas had a p_{CO}/p_{CO_2} ratio of 5 and pure CO was passed down the second tube at a flow rate of about $25 \, ml \, min^{-1}$.

The principal observations are summarized in the schematic, and somewhat idealized, figure 1. What appeared to be 'necklaces' of the oxidation product, presumed to be alumina, were generated at a regular frequency of 4–5 Hz. The average velocity of the expansion of the necklace was 120–$180 \, mm \, s^{-1}$ at a distance of about 10 mm
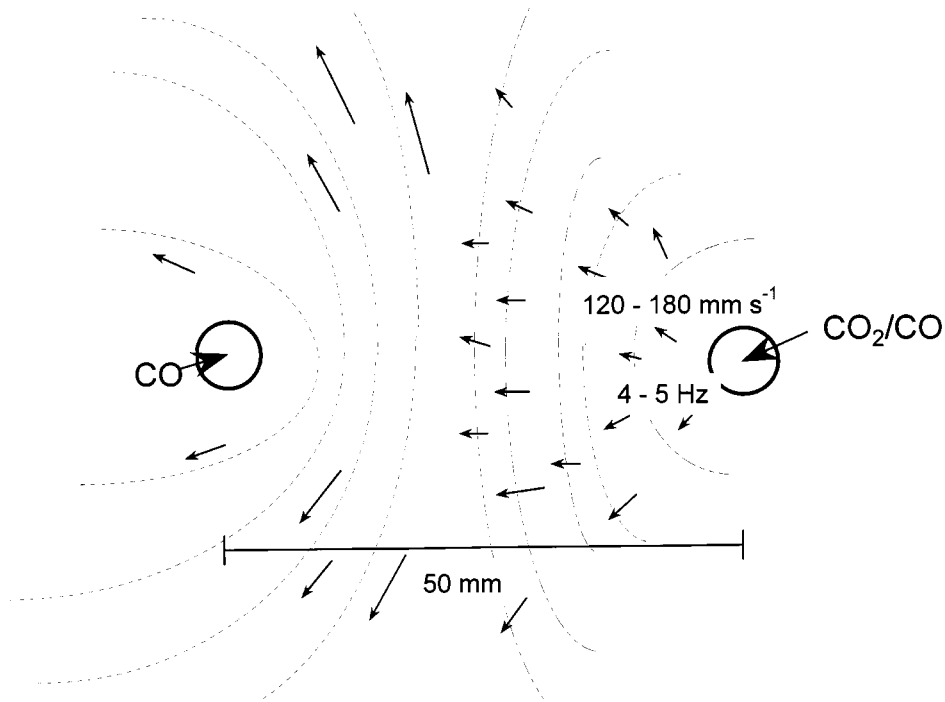
Figure 1. Schematic representation of the movement of 'necklaces' of alumina oxidation product in the experiments with the 0.019 wt% Al melt and a gas flow rate of 100 ml min^{-1}.
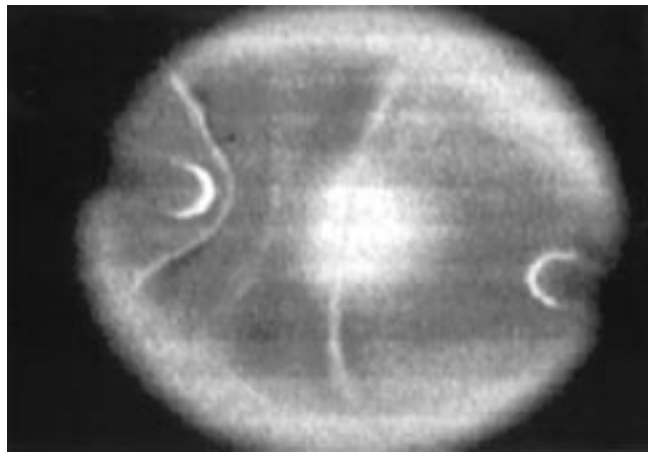

Figure 2. The expanding arc of the oxidation product, taken at a frame speed of 125 s^{-1}. The accumulation of oxidation product can be seen near the CO delivery tube on the left.

from the outer edge of the gas delivery tube. At a distance of 20–25 mm from the tube, the velocity was 60–80 mm s^{-1}. As the 'necklaces' approached to within about 10–15 mm of the CO gas delivery tube, motion towards the tube essentially stopped and particulate alumina moved towards the edges of the field of view. No pulsations were observed in the region of the CO delivery tube.

Figure 2 is from a single frame, taken at 125 s^{-1}. Although the resolution is poor, one expanding arc of the oxidation product is clear, as is the accumulation of the
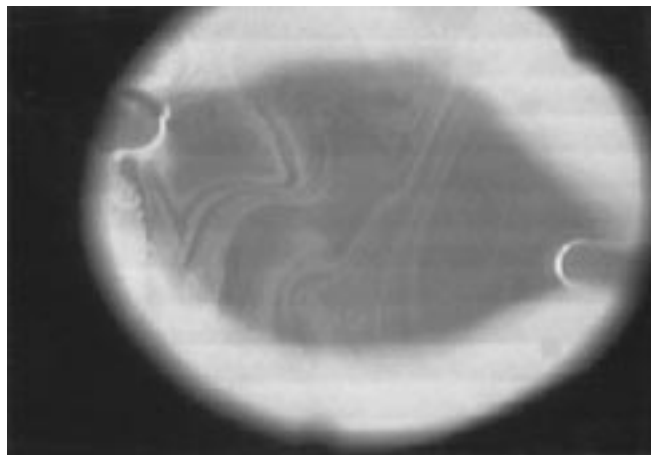
Figure 3. The accumulation of ribbons of oxidation product during an experiment with the 0.019 wt% Al melt during a period when a slow surface flow was occurring from left to right. The frame speed is $125\,\mathrm{s}^{-1}$.

product near to the CO delivery tube on the left-hand side. The white rings under the gas inlet tubes are reflected light from the bases of the tubes. Figure 3 is taken from a separate experiment where the glare was reduced. Although distorted by a slow drift of the surface of the liquid iron from left to right, presumably driven by a temperature gradient, the accumulation of ribbons of oxidation product is reasonably clear.

(*b*) *Lower aluminium-content melts with a low oxidizing gas flow rate*

A low flow rate of the oxidizing gas of 5–$7.5\,\mathrm{ml\,min}^{-1}$ was used in these experiments to minimize any effect of impinging jet momentum on the phenomena. In view of the low flow rate, the reaction gas was passed for several minutes before interrupting the power to the induction furnace. No gas was passed down the second tube. The carbon, manganese and silicon concentrations were 0.0010–0.0013, 0.40–0.41 and 0.13–0.14 wt%, respectively. Small additions of aluminium were made for each set of experiments and the resulting concentration of aluminium was successfully maintained at about 0.003 wt%. The initial melt had a very low sulphur concentration of 0.009 wt%. Additions of iron sulphide were made to give two additional melts of 0.056 and 0.21 wt% S.

Despite the low aluminium concentration, the expanding arcs could be seen clearly and alumina accumulated away from the inlet tube. Figure 4 is a close-up view of the area near to the gas inlet tube, taken at a frame rate of $250\,\mathrm{s}^{-1}$, from one of the experiments with the 0.2 wt% S melt and CO_2 as the oxidizing gas. The highlights on the expanding arc are consistent with the oblique illumination from the tip of the inlet tube being reflected by the moving surface disturbance.

Figure 5 shows, as the open circles, the pulsation frequency as a function of the CO_2/CO ratio in the oxidizing gas stream for the 0.009 wt% S melt. The two melts with higher sulphur concentrations at $p_{CO_2}/p_{CO} = \frac{1}{5}$ gave essentially the same value, as indicated by the open square. Within the experimental error, estimated to be about 10%, there appears to be no dependence on the sulphur concentration. The pulsation frequency for a pure CO_2 gas stream was greater than $2\,\mathrm{s}^{-1}$ for all of the sulphur concentrations, but the exact values could not be established with confidence.

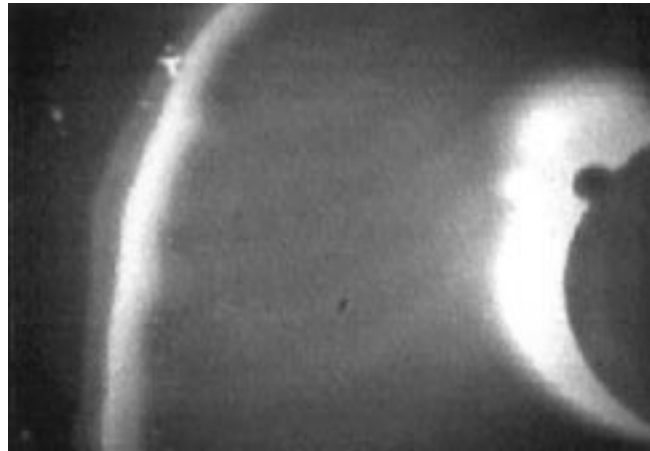Figure 6 shows the velocities of the 'necklaces' at approximately 10 mm from the

Figure 4. Close up view of the expanding arc, taken at a frame speed of $250\,\mathrm{s}^{-1}$, from an experiment with the 0.21 wt% S melt, showing what appears to be the surface disturbance, made visible by the oblique illumination from the tip of the gas inlet tube.
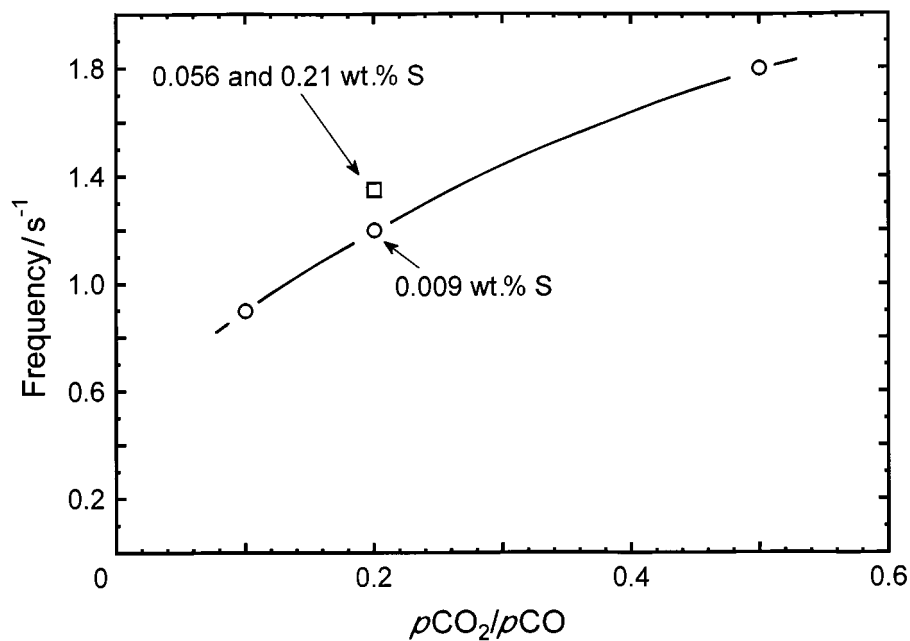

Figure 5. The pulsation frequency as a function of the CO_2/CO ratio in the gas stream for the 0.003 wt% Al melt at low gas low rates.

edge of the gas delivery tube as a function of the sulphur concentration for CO_2 and $p_{CO_2}/p_{CO} = \frac{1}{5}$ in the oxidizing gas stream. The experimental uncertainty in the velocity is estimated to be about 5%. There appears to be a distinct separation in the data and a clear reduction in the velocity with increasing sulphur concentration. The velocity observed in the experiments with high aluminium-content melts and high flow rates of the gas mixture with $p_{CO_2}/p_{CO} = \frac{1}{5}$ is shown by the closed circle in the same figure. There appears to be little difference in the velocity for the two conditions.
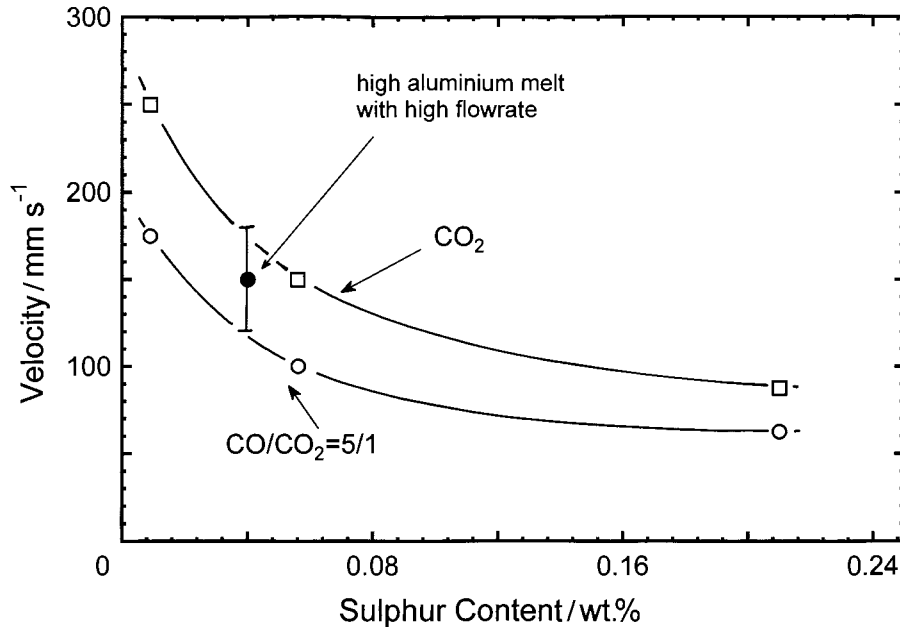
Figure 6. The velocities of movement at approximately 10 mm from the edge of the gas inlet tube in experiments with the 0.003 wt% Al melt and low gas flow rates.

In addition to the effect of sulphur on velocity, there was a marked tendency for the alumina oxidation product to form larger agglomerates at higher sulphur concentration. This can be seen by comparing figure 2 with figure 7, which is a sequence of frames, separated by 40 and 32 ms, in the order A → C, for experiments with CO_2 as the oxidizing gas and 0.21 wt% S in the steel. The larger agglomerates appear to be up to about 1 mm in diameter. Again, a slow drift of the surface from left to right was occurring during this particular sequence.

In the experiments with the low aluminium and highest sulphur content melts, irregular streaks appeared to follow the expanding arc. These can be clearly seen in figure 7c. From repeated observations, it is concluded that they most likely represented a second liquid phase which rapidly dissolved back into the bulk melt. Attempts to resolve this by the use of higher magnification ($\times 7$) were unsuccessful.

An addition of 0.04 wt% Se was made to the 0.21 wt% S melt to study the effect of a further decrease in the surface tension of the melt. Observations were made with a CO_2 reaction gas. Although pulsations of the surface near to the gas inlet tube occurred at an erratic frequency of about 1 Hz, no expanding 'necklaces' could be seen. Instead, a 'raft' of apparently solid oxidation product, approximately 5 mm in diameter, drifted from beneath the gas inlet tube at irregular intervals of 2–3 s. A detached 'raft' is shown in figure 8, where the tip of the gas inlet tube (8 mm OD) is at the right-hand side of the figure.

4. Discussion

(a) Origin of the phenomena

If the simplified case of liquid iron containing only aluminium as a deoxidant is considered, the reaction between the oxidizing gas stream and aluminium in a
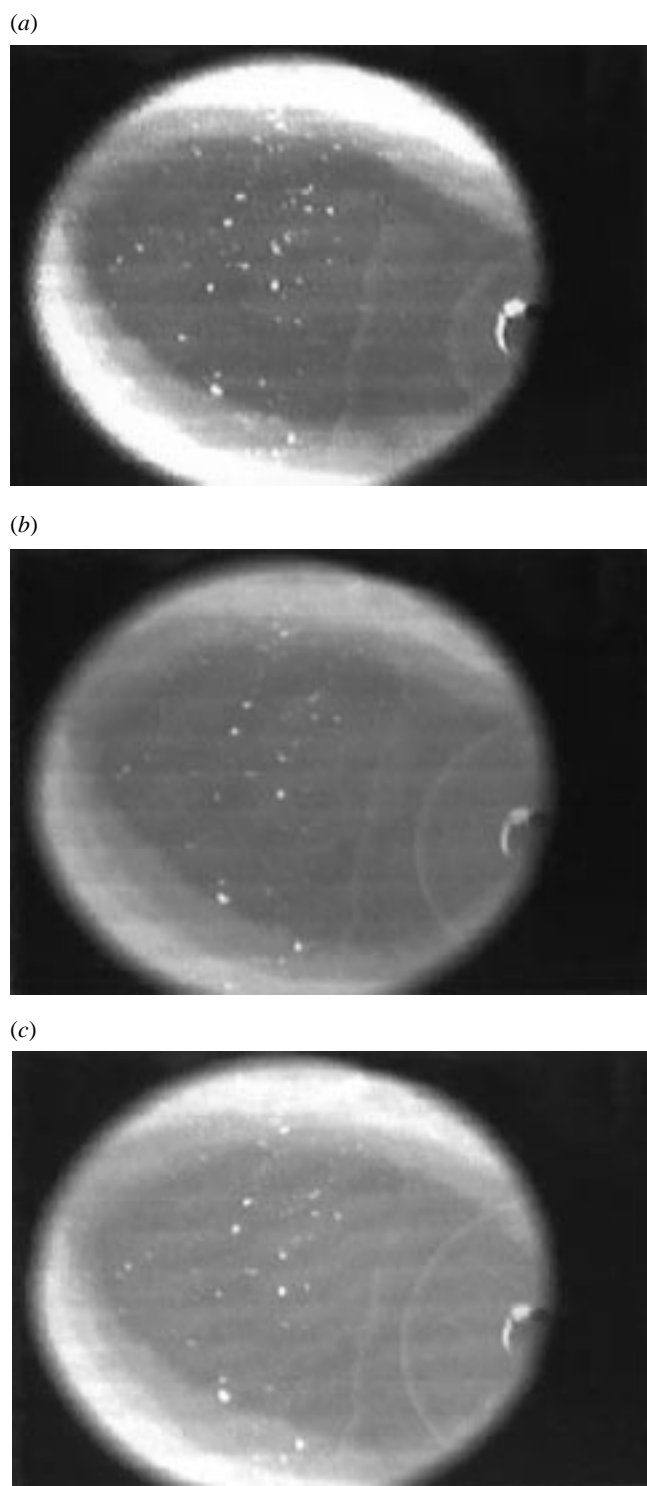
(*a*)

(*b*)

(*c*)

Figure 7. Sequence of frames (*a*)–(*c*), separated by 40 and 32 ms, in the order (*a*)–(*c*), from experiments with the 0.003 wt% Al melt with 0.21 wt% S at a low flow rate of CO_2 as the oxidizing gas.
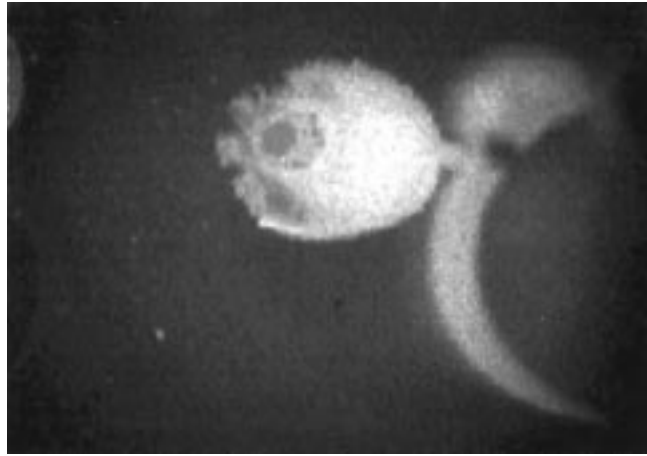
Figure 8. Detachment of a 'raft' of oxidation product from under the gas inlet tube during experiments with the 0.005 wt% Al melt containing 0.21 wt% S and 0.04 wt% Se with a low flow rate of CO_2. The frame speed is 500 s^{-1}.
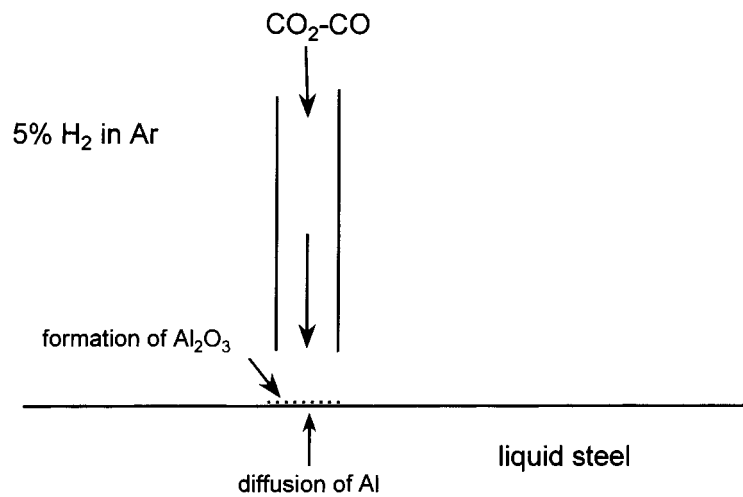

Figure 9. Schematic representation of the reaction between aluminium and the oxidizing gas stream, as assumed in the analysis.

stagnant melt may be represented schematically, as shown in figure 9. If there is no barrier to nucleation, alumina will be formed at the surface by the oxidation of aluminium diffusing from the bulk of the melt. For a constant flux of oxygen-containing species in the gas stream, and considering only one-dimensional diffusion, valid near to the centre line, the concentration of aluminium at the surface, C_S, will be given by

$$C_S = C_B - \frac{2Ft^{1/2}}{(D\pi)^{1/2}} \left(\frac{2}{3}\right), \tag{4.1}$$

where C_B is the concentration of aluminium in the bulk, F is the flux of oxygen atoms from the reacting gas species, D is the chemical diffusivity of aluminium and t is the elapsed time. The stoichiometric requirement is met by the factor $\left(\frac{2}{3}\right)$.

The aluminium concentration as a function of reduced time will follow the curve
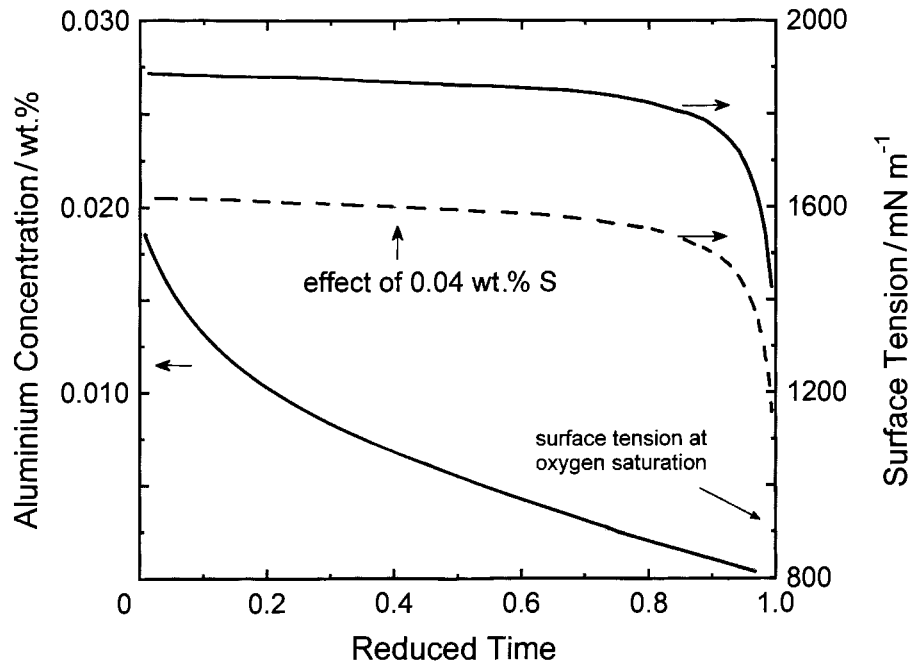
Figure 10. Calculated values of the aluminium concentration and surface tension below the centre of the gas inlet tube as a function of reduced time, from equations (4.1)–(4.3).

shown in figure 10. Turkdogan (1980) has shown that at concentrations of aluminium greater than 1 ppm, the deoxidation solubility product at $1600\,^\circ$C is given by

$$(a_{\mathrm{Al}})^2(a_{\mathrm{O}})^3 = 4.3 \times 10^{-14}, \tag{4.2}$$

where a_{Al} and a_{O} are the activities of aluminium and oxygen with respect to standard states of the 1 wt% ideal solutions. The surface tension of liquid iron as a function of the activity of oxygen at $1600\,^\circ$C, based on the work of Jimbo & Cramb (1992), is given by

$$\sigma = 1890 - 299\ln(1 + 100a_{\mathrm{O}}) \quad \mathrm{mN\,m^{-1}}. \tag{4.3}$$

Combination of equations (4.1)–(4.3) allows the calculation of the surface tension as a function of time. This is shown as a function of the reduced time in figure 10. Thus, following a small decrease in the surface tension for the bulk of the time, there is a sharp increase in the driving force for the radial flow of the liquid steel from under the impinging jet.

The local flux, F, of oxygen from the gas stream may be estimated from the modified Rao & Trass correlation due to Belton & Belton (1964) for impinging flow from a nozzle, namely,

$$Sh = 0.03Re^{1.06}\,Sc^{0.33}(x/d)^{-0.09}, \tag{4.4}$$

where the Sherwood number Sh is md/D, the Reynolds number Re is $\mathrm{d}u\rho/\mu$, the Schmidt number Sc is $\mu/\rho D$, x is the nozzle to surface distance, d is the inside diameter of the nozzle (tube), μ is the viscosity of the gas mixture, ρ is the density of the gas mixture, D is the interdiffusivity, u is the average velocity of the gas mixture and m is the mass transfer coefficient.

Taking the values of the transport properties of the gases from Turkdogan (1980), the derived value for the mass transfer coefficient of CO_2 is about $2.1\,\mathrm{cm\,s^{-1}}$ for the flow rate and gas composition of the first series of experiments. If $p_{CO_2} \to 0$ at the interface,

$$F = 1.4 \times 10^{-6}\,\mathrm{mol\,cm^{-2}\,s^{-1}}. \tag{4.5}$$

Substituting this value in equation (4.1), and taking the diffusivity of aluminium in liquid iron to be $5 \times 10^{-5}\,\mathrm{cm^2\,s^{-1}}$ from the recent work of Kawakami *et al.* (1997), leads to a value for t of 0.11 s for the condition $C_S \ll C_B$. Thus, following the radial dispersal of the oxidation product and low surface tension liquid, and the concomitant upward flow of fresh bulk liquid to the surface, the process would be expected to be successively repeated at a frequency of about 9 Hz.

Despite the approximations in this treatment, the order of magnitude agreement with the observed frequency of 4–5 Hz strongly suggests that the mechanism is essentially as described.

In view of the approximate additivity of the effects of oxygen and sulphur on the surface tension at low sulphur concentration (Ogino *et al.* 1983), discussed later, the effect of about 0.04 wt% S should be simply to lower the change in surface tension to that indicated by the dashed curve in figure 10. Similarly, the elapsed time is not strongly dependent on the 'end point'. If, for example, the dispersal of the alumina product occurs when the surface tension is depressed by $100\,\mathrm{mN\,m^{-1}}$ rather than by, say, $500\,\mathrm{mN\,m^{-1}}$, the shortening in the elapsed time would only be by about 10%.

The second series of experiments used very low flow rates of oxidizing gas, well below the range of applicability of the correlation (equation (4.4)). Linear gas velocities were in the range of only $0.5\text{--}1.0\,\mathrm{cm\,s^{-1}}$. Accordingly, it is not possible to make an experimentally well-established estimate of the flux of oxygen to the surface of the melt. However, the oxidation appears to be confined to the region directly under the gas inlet tube, as indicated by the size of the 'raft' of oxidation product in figure 8.

If, to a very first approximation, the average flux of oxygen to the surface, F, is taken as proportional to the volume flow rate of the gas, the ratio of the flux in the second series of experiments to that in the first series of experiments at $p_{CO_2}/p_{CO} = \frac{1}{5}$ would be about 0.07. The bulk concentration of aluminium, C_B, is about 0.003 wt%. According to equation (4.1), the pulsation frequency, $1/t$, should therefore be about 2 Hz, i.e. reduced by a factor of about 5. The observed frequency for these conditions (figure 5) was about 1.2 Hz. Thus, the lowering of the pulsation frequency is reasonably consistent with the proposed mechanism.

Within the experimental error, there was no effect of sulphur concentration on the pulsation frequency at $p_{CO_2}/p_{CO} = \frac{1}{5}$, as shown in figure 5. Belton (1993) has shown that sulphur markedly decreases the interfacial rate of dissociation of CO_2 on liquid iron, this observation is consistent with the transport of oxygen to the surface being dominated by physical mass transfer processes, as assumed in analysis.

(b) *The velocity of motion and the effects of changes in bulk surface tension*

The effect of the concentration of sulphur on the surface tension of liquid iron at 1550–1600 °C, based upon the bulk of the available experimental data, has been shown by Belton (1976) to be described by the equation

$$\sigma = 1778 = 195 \ln(1 + 185 a_S) \quad \mathrm{mN\,m^{-1}}, \tag{4.6}$$

where a_S is the activity of sulphur with a standard state of the 1 wt% ideal solution. Neglecting the relatively small effects of the other solutes on the activity coefficient
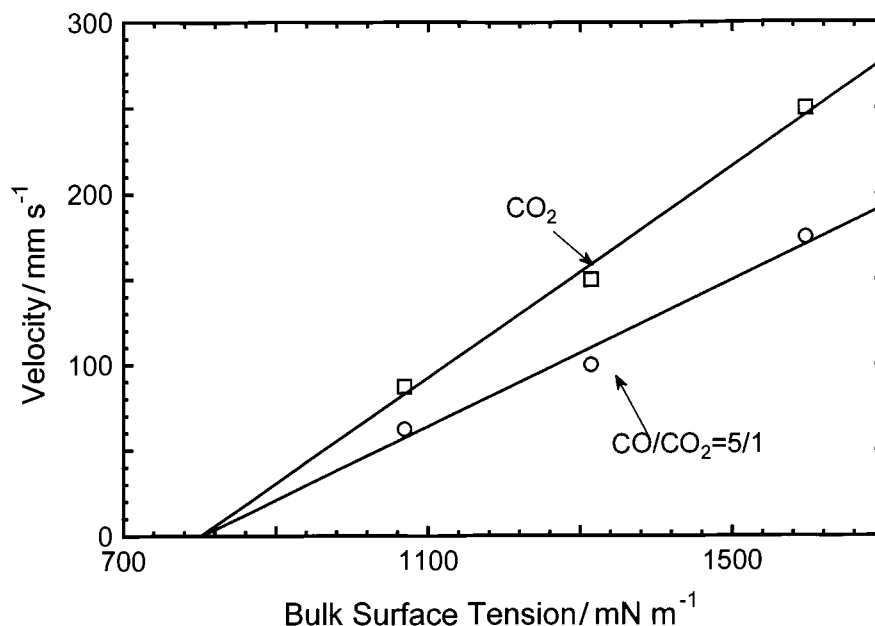
Figure 11. Velocities of the front movement at 10 mm from the edge of the gas inlet tube as a function of the calculated bulk surface tension for the experiments with the 0.003 wt% Al melt.

of sulphur, the results in figure 6 may therefore be converted to a plot of the observed velocity versus the surface tension of the bulk liquid iron, as shown in figure 11. The results for both oxidizing conditions appear to extrapolate to zero velocity at about 800 mN m^{-1}.

Naidich & Zabuga (1992) have derived the following expression for the Marangoni-driven velocity of front movement when a droplet, enriched with a surface active solute, is introduced to the surface of a liquid:

$$v = (\Delta\sigma^2/4\alpha^2\mu\rho r)^{1/3}, \tag{4.7}$$

where α is a constant equal to 0.332, $\Delta\sigma$ is the difference in surface tension between the bulk liquid and the droplet, μ and ρ are the viscosity and density of the liquid, and r is the distance between the moving front and the source. Reasonably good agreement was found between observed and calculated velocities for experiments with water and surfactant-enriched droplets.

Hirashima *et al.* (1995) have recently used computation fluid dynamics to model the continuous Marangoni-induced flow caused by the dissolution of nitrogen into liquid iron from an impinging jet. Agreement between their measured and calculated velocities was obtained when an effective viscosity, defined by

$$\mu_{\text{eff}} = \mu + \mu_{\text{t}}, \tag{4.8}$$

was used in the computation, where μ_{t} is the turbulent viscosity, taken to be about 5μ. This was considered to be reasonable for mildly turbulent flow.

Taking the value of μ to be $5 \times 10^{-3} \text{ Pa s}$, and assuming a similar multiplicative factor for the turbulent viscosity, substitution in equation (4.7) leads to

$$v \approx 1.03(\Delta\sigma)^{2/3} \quad \text{m s}^{-1} \tag{4.9}$$

at a distance of 10 mm from the source, when the units for $\Delta\sigma$ are N m^{-1}.

The trend of decreasing velocity with decreasing bulk surface tension in figure 11 is therefore to be expected if $\Delta\sigma$ similarly decreases. There is experimental evidence that this is true for a given change in oxygen activity. Gaye *et al.* (1984) have shown that at a sulphur concentration of about 0.1 wt% or above, the further depression of the surface tension caused by increasing the oxygen activity from *ca.* 0 to 0.004 is hardly detectable. Whereas, at very low sulphur concentration (less than 0.03 wt%), the effects of oxygen and sulphur have been found to be approximately additive (Ogino *et al.* 1983).

The extrapolation to zero velocity at a bulk surface tension of about $800\ \mathrm{mN\ m^{-1}}$ suggests that this is the region where an increase in the activity of oxygen has no significant effect on the surface tension. Unfortunately, there have been no independent studies of the effect of high activities of oxygen on the surface tension of liquid iron at high sulphur concentrations. Kozakevitch & Urbain (1961) reported that the addition of 0.04 wt% of selenium to liquid iron reduces the surface tension to about $1000\ \mathrm{mN\ m^{-1}}$. The quantitative effect of the addition of this amount to the 0.2 wt% S melt has not been experimentally determined, but it is reasonable to expect that the resulting surface tension would be significantly below $1000\ \mathrm{mN\ m^{-1}}$. The observation that the 'raft' of oxidation product did not disperse under these conditions is consistent with the driving force, $\Delta\sigma$, being very small.

If it is assumed that the dispersal of the alumina occurs just before the nucleation of a liquid manganese–silicate oxidation product, the maximum activity of oxygen would be about 0.015 (Turkdogan 1980). At low sulphur concentration, the depression of the surface tension can be estimated from equation (4.3) to be about $270\ \mathrm{mN\ m^{-1}}$. Substitution of this in equation (4.9) gives an expected velocity of movement of the front of about $0.43\ \mathrm{m\ s^{-1}}$ at a distance of 10 mm from the source. This is to be compared with the observed values for the 0.009 wt% S melt of about $0.25\ \mathrm{m\ s^{-1}}$ for CO_2 as the oxidizing gas, and $0.16\ \mathrm{m\ s^{-1}}$ for $p_{CO_2}/p_{CO} = \frac{1}{5}$. Thus the magnitude of the velocity is reasonably consistent with the assumptions, if equation (4.7) is accepted.

The observed increase in the velocity by a factor of about 1.5 for a six-fold increase in the partial pressure of CO_2 in the gas stream suggests that there is some sensitivity of the activity of oxygen, and hence $\Delta\sigma$, at the point of dispersal of the oxidation product on the flux of oxygen to the surface. Neglecting the uncertainties in the measurements, a change in the end-point activity of oxygen by a factor of about two would account for the difference for the low sulphur melt, if the value of $\Delta\sigma$ is of the order of $102\ \mathrm{mN\ m^{-1}}$. However, the similarity of the velocity at a given concentration of sulphur between the first and second series of experiments is consistent with the bulk surface tension being the most important factor in establishing the velocity under the conditions of the experiments.

5. Conclusion

Consistent with the observations, the foregoing analysis has contained the assumption that the 'raft' of alumina oxidation product remains intact under the gas delivery tube until the Marangoni driving force is sufficient to cause the sudden dispersion. It has been shown recently by Emi *et al.* (1997) and Yin *et al.* (1997) that relatively long-range ($\leqslant 50\ \mu\mathrm{m}$) forces exist, probably due to capillary effects, between alumina particles on the surface of liquid iron. These cause the particles to agglomerate.

It appears likely that these are the forces that prevent the random dispersal of the alumina until possibly a critical value of $\Delta\sigma$ is exceeded.

References

Belton, G. R. 1976 *Metall. Trans.* B **7**, 35–42.

Belton, G. R. 1993 *Metall. Trans.* B **24**, 241–258.

Belton, G. R. & Belton, R. A. 1980 *Trans. Iron Steel Inst. Jap.* **20**, 87–91.

Emi, T., Yin, H. & Shibata, H. 1997 *CAMP-ISIJ* **10**, 93–96.

Gaye, H., Lucas, L.-D., Olette, M. & Riboud, P. V. 1984 *Can. Met. Q.* **23**, 179–191.

Hammerschmid, P. 1987 *Stahl Eisen* **107**, 35–40.

Hirashima, N., Choo, R. T. C., Toguri, J. M. & Mukai, K. 1995 *Metall. Mater. Trans.* B **26**, 971–980.

Jimbo, I. & Cramb, A. W. 1992 *ISIJ Int.* **32**, 26–35.

Kawakami, M., Yokoyama, S., Takagi, K., Nishimura, M. & Kim, J.-S. 1997 *ISIJ Int.* **37**, 425–431.

Kozakevitch, P. & Urbain, G. 1961 *Mem. Sci. Rev. Met.* **58**, 517–534.

Mukai, K. 1992 *ISIJ Int.* **42**, 19–25.

Naidich, Yu. V. & Zabuga, V. V. 1992 *Metally* no. 4, 40–46.

Ogino, K., Nogi, K. & Hosoi, C. 1983 *Tetsu-to-Hagane* **69**, 1988–1994.

Olette, M. 1993 *ISIJ Int.* **33**, 1113–1124.

Rao, V. V. & Trass, O. 1964 *Can. J. Chem. Engng* **42**, 95–99.

Sigworth, G. K. & Elliott, J. F. 1974 *Met. Sci.* **8**, 298–310.

Turkdogan, E. T. 1980 *Physical chemistry of high temperature technology.* New York: Academic.

Yin, H., Shibata, H., Emi, T. & Suzuki, M. 1997 *ISIJ Int.* **37**, 936–945.